Court and spark in the wild: communication at the limits of sensation

Jörg Henninger[1], Frank Kirschbaum[2], Jan Grewe[1], Rüdiger Krahe[3], Jan Benda[1*]

[1]Institut für Neurobiologie, Eberhard Karls Universität, Auf der Morgenstelle 28E, 72076 Tübingen, Germany

[2]Lebenswissenschaftliche Fakultät, Humboldt-Universität zu Berlin, Philippstr. 13, Haus 16, 10115 Berlin, Germany

[3]McGill University, Department of Biology, 1205 Docteur Penfield, Montreal, Quebec H3A 1B1, Canada

[*]Correspondence to: jan.benda@uni-tuebingen.de

Summary

Sensory systems evolve for processing complex natural scenes [1] in order to generate successful behavior. Consequently, natural-like stimuli have been crucial for recent advances in understanding the design and function of neural circuits in sensory systems (e.g., visual: [2, 3], auditory: [4, 5, 6]). Communication signals are by definition an important class of natural stimuli. Acoustic communication signals have been reported to evoke responses in peripheral auditory neurons that are highly informative about these stimuli [7, 8]. However, other stimulus ensembles that do not optimally drive sensory neurons can also be behaviorally relevant and equally important for understanding the functioning of neural systems. Unfortunately, they are often neglected [9]. By tracking electrocommunication behavior of weakly electric fish in their Neotropical habitat, we found frequent courtship and aggressive interactions that non-optimally drive sensory neurons just above their threshold. Nevertheless, these weak signals elicited reliable behavioral responses, such as echo-responses to communication signals (so called "chirps"), synchronization of spawning by a tightly coordinated chirp interaction between male and female fish, and long-range attacks on intruding males. Surprisingly, abundant electrosensory signaling during courtship behaviors occur at the limits of the electroreceptors' frequency tuning. Electrosensory stimuli during male-male interactions match receptor tuning much better, but many attacks are triggered at large inter-male distances when stimuli are exceedingly weak. Our findings demonstrate that the statistics of species-specific natural stimuli measured in the natural habitat might reveal unexpected behaviorally relevant scenes that are successfully processed by the neural system despite non-optimal activation of sensory neurons.

Results and Discussion

We took advantage of the continuously generated electric organ discharge (EOD; Fig. 1 a) of gymnotiform weakly electric fish, an integral part of their active sensory system [10], that allows to track their movements and communication signals without the need of tagging individual fish. We continuously recorded EODs of weakly electric fish in a stream in the Panamanian rainforest by means of a submerged electrode array (Fig. S1, Fig. 1 b, movie S6, and Supplemental experimental procedures). Individual gymnotiform knifefish, *Apteronotus rostratus*, were tracked based on the individual-specific frequency of their quasi-sinusoidal EOD (EODf=600–1200 Hz) during their reproductive season. In the recordings we detected several types of electro-communication signals — brief EOD frequency excursions called "chirps" emitted during courtship and aggression (Fig. 1 c, [11]). This approach allowed us to reconstruct social interactions in detail (Fig. 1 d–f, movies S7 and S8, and Supplemental experimental procedures) and evaluate the associated sensory scenes experienced by these fish in their natural habitat.

We focused on two relevant communication behaviors, i.e., courtship and aggressive dyadic interactions. In total, we detected 54 episodes of short-distance interactions that we interpreted as courtship (see below) between low-frequency females (EODf < 750 Hz) and high-frequency males (EODf > 750 Hz), occurring exclusively at night. Courting was characterized by extensive production of chirps (Fig. 1 d) by both males and females — with up to 8 400 chirps per fish per night (Fig. S2). Most chirps were so-called "small chirps", characterized by short duration (< 20 ms) EODf excursions of less than 150 Hz and minimal reduction in EOD amplitude [12] (Fig. 1 c). In courtship episodes only females emitted an additional type of chirp, the "long chirp" (Fig. 1 c and Supplementary Information), with a duration of 162 ± 39 ms (n = 54), a large EODf excursion of about 400 Hz, and a strong decrease in EOD amplitude. Per night and female we observed 9 to 45 long chirps generated every 3 to 9 minutes (1st and 3rd quartile), exclusively between 7 pm and 1 am (Fig. S2). Occasionally, courtship was interrupted by intruding males, leading to aggressive interactions (Fig. 1 d–f, movies S7 and S8 show examples of such behaviors).

We found that courtship communication was highly structured, with female long chirps playing a central role. Long chirps were preceded by persistent emission of small chirps by the male with rates of up to 3 Hz (Figs. 2 a and S4 a), exceeding maximum small-chirp rates reported from laboratory observations [12, 13]. Immediately before the long chirp, the female small-chirp rate tripled from below 1 Hz to about 3 Hz within a few seconds. The male chirp rate followed this increase until the concurrent high-frequency chirping of both fish ceased after the female long chirp. These chirp episodes were characterized by close proximity of the two fish (< 30 cm, Figs. 2 b and S4 b). Long chirps were consistently acknowledged by males with a doublet of small chirps emitted 229 ± 31 ms after long chirp onset (Fig. 2 c). The two chirps of the doublet were separated by only 46 ± 6 ms, more than seven-fold shorter than the most prevalent chirp intervals (Fig. S3). The concurrent increase in chirp rate and its termination by the female long chirp and male doublet stood out as a highly stereotyped communication motif that clearly indicates fast interactive communication (Fig. 2 c, audio S5).

On a sub-second timescale, male chirping was modulated by the timing of female chirps (Figs. 2 d and Fig. S4 c). Following a female small chirp, male chirp probability first decreased to a minimum at about 75 ms (n = 5 pairs of fish) and subsequently increased to a peak at about 165 ms. The precise timing of this echo response demonstrates responsive communication and supports the functional relevance of chirping as a communication signal. In contrast to males, females did not show any echo response (Figs. 2 e and Fig. S4 d) — they timed their chirps independently of the males' chirps. Previous lab studies found slower echo responses exclusively between males [13, 14, 15] and inhibiting effects of small chirps on attack behavior [16].

External fertilizers among aquatic animals often employ communication signals, e.g., visual

and/or tactile, to synchronize egg spawning and sperm release and ensure fertilization, e.g. [17]. The repeated occurrence of stereotypical communication sequences and close-proximity movement in our recordings suggested a synchronizing function of chirping in egg spawning [18]. We tested this hypothesis in a breeding experiment in the laboratory [19] by continuously recording and videotaping a group of 3 males and 3 females of the closely related species *A. leptorhynchus* [20] over more than 5 months (Supplemental experimental procedures). Scanning more than 1.3 million emitted chirps, we found 76 female long chirps embedded in communication episodes similar to those observed in *A. rostratus* in the wild. Eggs were only found after nights with long chirps (six nights). In addition, the associated video sequences triggered on female long chirps clearly demonstrate the exclusive function of the female long chirp in synchronizing spawning and external fertilization, and emphasize the behavioral relevance of these interactions (Fig. 3, movie S9).

A second common type of electro-communication interaction was aggressive encounters between males competing for access to reproductively active females. These aggressive interactions were triggered by intruding males that disrupted courtship of a resident, courting dyad. The resident males then usually attacked the intruder, showing a clear onset of directed movement toward the intruder (Fig. 1 e, movie S7). In 5 out of 12 such situations a few small chirps indistinguishable from those produced during courtship were elicited exclusively by the retreating fish (Fig. S2), suggesting an additional, possibly submissive function of small chirps in aggressive contexts [13, 21].

Our observations on chirping in free-living A. rostratus and reproductive A. leptorhynchus in the lab are at odds with previous assumptions on natural communication behavior of *Apteronotus*. E.g., small chirps were assumed to be emitted predominantly among males [12, 13]. In contrast, in our data of both *A. leptorhynchus* and *A. rostratus*, small chirps were emitted in large quantities by courting males and females and only occasionally during aggressive encounters.

In a final step, we deduce the statistics of natural electrosensory stimuli resulting from the observed communication behaviors and relate it to the known properties of electrosensory physiology. Superposition of a fish's EOD with that of a nearby fish results in a periodic amplitude modulation, a so-called beat. Both frequency and amplitude of the beat provide a crucial signal background for the neural encoding of communication signals. The beat frequency is given by the difference between the two EODf and the beat amplitude equals the EOD amplitude of the nearby fish at the position of the receiving fish [22] (Fig. 4 a). The amplitude modulations are encoded by tuberous electroreceptors (P-units) distributed over the fish's skin [23, 24, 25, 26, 27].

We estimated the population activity of P-unit afferents in *A. leptorhynchus* from the standard deviation of the summed nerve activity (Supplemental experimental procedures), which is known to closely match the tuning properties of single nerve fibers [26, 27]. The P-unit population response quickly dropped to low signal-to-noise ratios (Cohen's $d < 1$) at inter-fish distances larger than about 30 cm at 60 Hz beat frequency (Fig. 4 b). P-unit afferents are also tuned to beat frequency and are most sensitive between 30–130 Hz[23, 25, 26, 27] (Fig. 4 e), covering the beat frequencies arising from same-sex interactions (Fig. 4 h). Remarkably, all courtship chirping occurred at much higher beat frequencies (205–415 Hz, Fig. 4 g). Even though the beat amplitudes during these interactions are large, because of the small distances of less than 32 cm (Fig. 4 c), such high-frequency stimuli evoke weak P-unit activity ($d < 0.83$ at the closest measured distance for 260 Hz beat frequency), which, nevertheless, must be the basis of the observed precisely timed chirp interactions. The probability to encounter these high beat frequencies is similar to the probability of low beat frequencies typical for same-sex interactions (Fig. 4 f). This stimulus distribution and the obvious relevance of high frequency stimuli for male-female communication is not reflected by the very low and flat tuning curve of the receptors in the high frequency range, indicating a non-optimal representation of these signals (see Supplemental information). The profound mismatch between the tuning of recep-

tor neurons and the high beat frequencies occurring during courtship is unexpected given the many examples of optimally encoded courtship signals in other sensory systems, e.g. [8, 28]. This mismatch is also unexpected from the perspective of the design of animal communication systems [29] and points to additional selective forces.

In contrast, two behaviors involving intruding males occurred within the P-units' best-frequency range (Fig. 4 h), but at much larger distances (Fig. 4 d): (i) Intruding males initially often lingered at distances larger than 70 cm from the interacting dyad (8 of 16 scenes, median duration 58.5 s; e.g., Fig. 1 d, movie S7), consistent with assessment behavior [30]. (ii) The distances at which resident males started to attack intruders ranged from 20 cm to 177 cm (81 ± 44 cm, $n = 10$, Fig. 1 d, movie S8). At the largest observed attack distance of 177 cm, the electric field strength was estimated to be maximally 0.34 µV/cm – assuming the fish were oriented optimally – a value close to minimum behavioral threshold values of about 0.1 µV/cm measured in the laboratory at the fish's best frequency [31, 32]. Both types of aggression behaviors therefore evoke weak activity of P-units close to the fish's perception threshold.

In contrast to previous findings of an optimal tuning of peripheral neurons to natural stimuli [8, 33] we here observed relevant behaviors that systematically evoke only weak, non-optimal neural responses. Male echo responses occurring reliably within a few tens of milliseconds, precisely timed chirp doublets, and long-range attacks (Fig. 4 c, d) demonstrate that the respective electrocommunication signals are successfully and robustly evaluated by the electrosensory system despite the weak effective receptor activation that these interactions generate. These robust behavioral performances suggest highly sensitive detection mechanisms in central sensory processing. Such mechanisms likely involve feedback connections from higher brain areas, including the telencephalon [34, 35], that modulate the first stage of electrosensory processing in the hindbrain [36].

We attribute our identification of behaviors at the limits of sensation to the natural setting of our measurements. Our results strongly emphasize the importance of the ethological perspective for identifying the real challenges faced and solved by sensory systems by quantifying species-specific natural behavior and linking it to sensory physiology.

Author contributions

J.H. developed the equipment for field recordings of electric fish, J.H., J.B. and R.K. acquired field recordings, J.H. developed the software for electric fish tracking and analyzed behavioral data, J.G. and J.B. recorded electrophysiological data, J.H. and F.K. performed the breeding study, J.B. designed the study, J.H., J.G., R.K., J.B. wrote the manuscript.

Acknowledgments

Supported by the BMBF Bernstein Award Computational Neuroscience 01GQ0802 to J.B., a Discovery Grant from the Natural Sciences and Engineering Research Council of Canada to RK, and a Short Time Fellowship to J.H. from the Smithonian Tropical Research Institute. We thank Hans Reiner Polder and Jürgen Planck from npi electronic GmbH for designing the amplifier, Sophie Picq, Diana Sharpe, Luis de León Reyna, Rigoberto González, Eldredge Bermingham, the staff from the Smithsonian Tropical Research Institute, and the Emberá community of Peña Bijagual for their logistical support, Fabian Sinz for advice on the analysis, and Ulrich Schnitzler, Len Maler, and Janez Presern for comments on the manuscript.

References

[1] Lewicki, M., Olshausen, B., Surlykke, A., and Moss, C. (2014). Scene analysis in the natural environment. *Front Psychol* 5, pp. 1–21.

[2] Olshausen, B. and Field, D. (1996). Emergence of simple-cell receptive-field properties by learning a sparse code for natural images. *Nature* 381, pp. 607–609.

[3] Gollisch, T. and Meister, M. (2010). Eye smarter than scientists believed: neural computations in circuits of the retina. *Neuron* 65.2, pp. 150–164.

[4] Theunissen, F. E., Sen, K., and Doupe, A. J. (2000). Spectral-temporal receptive fields of nonlinear auditory neurons obtained using natural sounds. *The Journal of Neuroscience* 20.6, pp. 2315–2331.

[5] Smith, E. and Lewicki, M. (2006). Efficient auditory coding. *Nature* 439.7079, pp. 978–982.

[6] Clemens, J. and Ronacher, B. (2013). Feature Extraction and Integration Underlying Perceptual Decision Making during Courtship Behavior. *J Neurosci* 33.29, pp. 12136–12145.

[7] Rieke, F., Bodnar, D. A., and Bialek, W. (1995). Naturalistic stimuli increase the rate and efficiency of information transmission by primary auditory afferents. *Proc. R. Soc. Lond. B* 262, pp. 259–265.

[8] Machens, C., Gollisch, T., Kolesnikova, O., and Herz, A. (2005). Testing the efficiency of sensory coding with optimal stimulus ensembles. *Neuron* 47.3, pp. 447–456.

[9] Olshausen, B. A. and Field, D. J. (2005). How Close Are We to Understanding V1?. *Neural Comput.* 17, pp. 1665–1699.

[10] Heiligenberg, W. (1991). *Neural nets in electric fish.* Cambridge, MA: MIT Press.

[11] Zakon, H., Oestreich, J., Tallarovic, S., and Triefenbach, F. (2002). EOD modulations of brown ghost electric fish: JARs, chirps, rises, and dips. *J Physiol Paris* 96.5–6, pp. 451–458.

[12] Engler, G. and Zupanc, G. (2001). Differential production of chirping behavior evoked by electrical stimulation of the weakly electric fish, *Apteronotus leptorhynchus*. *J Comp Physiol A* 187.9, pp. 747–756.

[13] Hupé, G. J. and Lewis, J. E. (2008). Electrocommunication signals in free swimming brown ghost knifefish, *Apteronotus leptorhynchus*. *J Exp Biol* 211.Pt 10, pp. 1657–1667.

[14] Zupanc, G., Sîrbulescu, R., Nichols, A., and Ilies, I. (2006). Electric interactions through chirping behavior in the weakly electric fish, *Apteronotus leptorhynchus*. *J Comp Physiol A* 192.2, pp. 159–173.

[15] Salgado, J. and Zupanc, G. (2011). Echo response to chirping in the weakly electric brown ghost knifefish (*Apteronotus leptorhynchus*): role of frequency and amplitude modulations . *Can J Zool* 89, pp. 498–508.

[16] Walz, H., Hupé, G., Benda, J., and Lewis, J. (2013). The neuroethology of electrocommunication: how signal background influences sensory encoding and behaviour in *Apteronotus leptorhynchus*. *J Physiol Paris* 107.1, pp. 13–25.

[17] Lobel, P. (1992). Sounds produced by spawning fishes. *Environ Biol Fishes* 33.4, pp. 351–358.

[18] Hagedorn, M. and Heiligenberg, W. (1985). Court and spark: electric signals in the courtship and mating of gymnotid fish. *Anim Behav* 33, pp. 254–265.

[19] Kirschbaum, F. and Schugardt, C. (2002). Reproductive strategies and developmental aspects in mormyrid and gymnotiform fishes. *J Physiol Paris* 96, pp. 557–566.

[20] de Santana, C. D. and Vari, R. P. (2013). Brown ghost electric fishes of the *Apteronotus leptorhynchus* species-group (Ostariophysi, Gymnotiformes); monophyly, major clades, and revision. *Zool J Linnean Soc* 168, pp. 564–596.

[21] Smith, G. (2013). Evolution and hormonal regulation of sex differences in the electrocommunication behavior of ghost knifefishes (Apteronotidae). *J Exp Biol* 216, pp. 2421–33.

[22] Fotowat, H., Harrison, R., and Krahe, R. (2013). Statistics of the electrosensory input in the freely swimming weakly electric fish *Apteronotus leptorhynchus*. *J Neurosci* 33.34, pp. 13758–13772.

[23] Bastian, J. (1981). Electrolocation I. How Electroreceptors of *Apteronotus albifrons* Code for Moving Objects and Other Electrical Stimuli. *J Comp Physiol* 144, pp. 465–479.

[24] Carr, C. E., Maler, L., and Sas, E. (1982). Peripheral organization and central projections of the electrosensory nerves in gymnotiform fish. *J Comp Neurol* 211, pp. 139–153.

[25] Nelson, M., Xu, Z., and Payne, J. (1997). Characterization and modeling of P-type electrosensory afferent responses to amplitude modulations in a wave-type electric fish. *J Comp Physiol A* 181, pp. 532–544.

[26] Benda, J., Longtin, A., and Maler, L. (2006). A Synchronization-Desynchronization Code for Natural Communication Signals. *Neuron* 52, pp. 347–358.

[27] Walz, H., Grewe, J., and Benda, J. (2014). Static frequency tuning properties account for changes in neural synchrony evoked by transient communication signals. *J Neurophysiol* 112, pp. 752–765.

[28] Schrode, K. and Bee, M. (2015). Evolutionary adaptations for the temporal processing of natural sounds by the anuran peripheral auditory system. *J Exp Biol* 218.6, pp. 837–848.

[29] Bradbury, J. and Vehrencamp, S. (2011). *Principles of animal communication*. 2nd. Sunderland: Sinauer.

[30] Arnott, G. and Elwood, R. (2008). Information gathering and decision making about resource value in animal contests. *Anim Behav* 76, pp. 529–542.

[31] Knudsen, E. (1974). Behavioral thresholds to electric signals in high frequency electric fish. *J Comp Physiol A* 91.4, pp. 333–353.

[32] Bullock, T., H, R., and Scheich, H. (1972). The jamming avoidance response of high frequency electric fish. II. Quantitative aspects. *J Comp Physiol* 77.1, pp. 23–48.

[33] Laughlin, S. (1981). A simple coding procedure enhances a neuron's information capacity. *Z. Naturforsch. C* 36.9-10, pp. 910–912.

[34] Giassi, A. C., Duarte, T. T., Ellis, W., and Maler, L. (2012). Organization of the Gymnotiform Fish Pallium in Relation to Learning and Memory: II. Extrinsic Connections. *J Comp Neurol* 520, pp. 3338–3368.

[35] Krahe, R. and Maler, L. (2014). Neural maps in the electrosensory system of weakly electric fish. *Curr Opin Neurobiol* 24, pp. 13–21.

[36] Bastian, J. (1986). Gain Control in the Electrosensory System Mediated by Descending Inputs to the Electrosensory Lateral Line Lobe. *J Neurosci* 6.2, pp. 553–562.

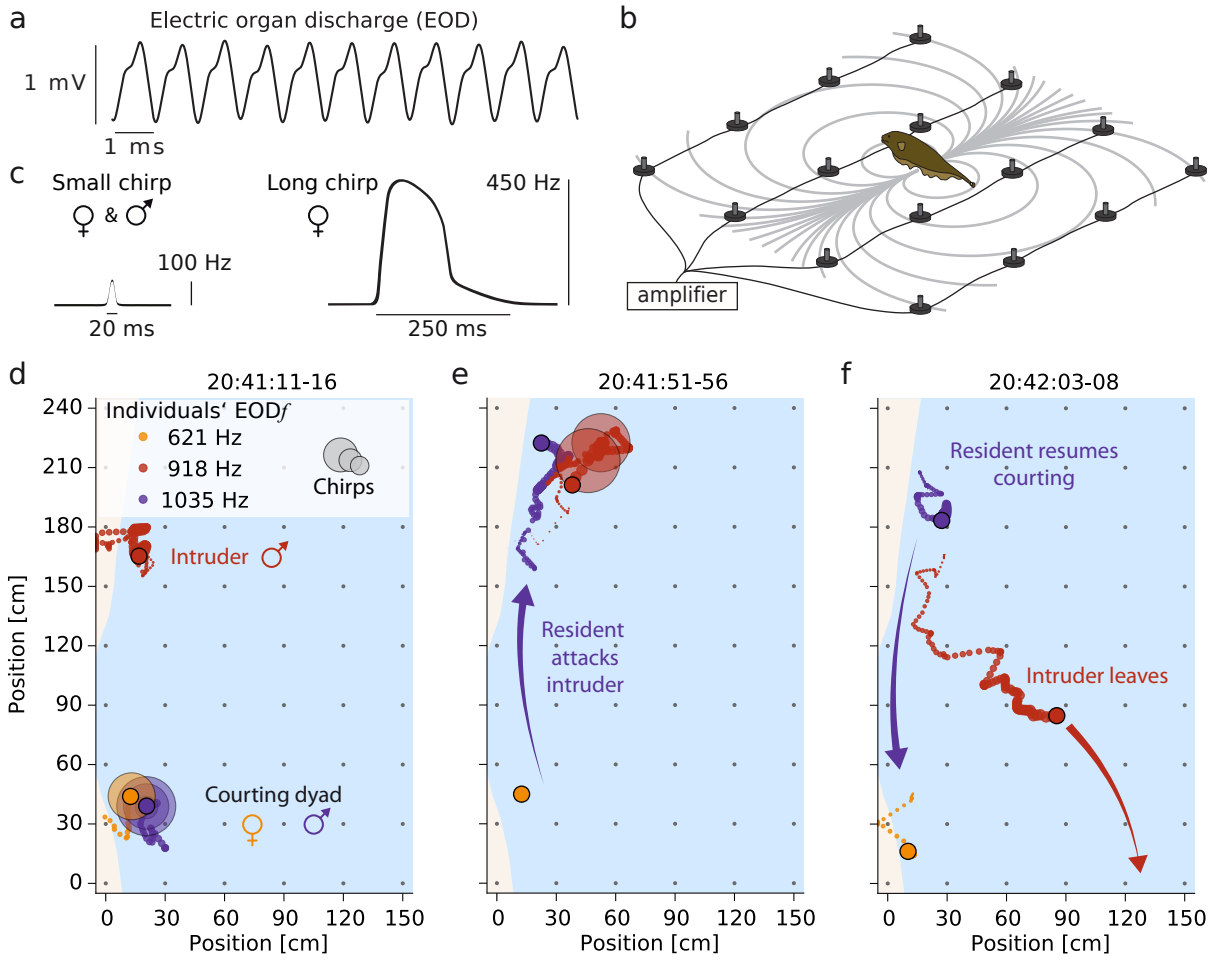

Figure 1: Monitoring electrocommunication behavior in the natural habitat. a) EOD waveform of *A. rostratus*. b) The EOD generates a dipolar electric field (gray isopotential lines) that we recorded with an electrode array. c) Transient increases of EOD frequency, called small and long chirps, function as communication signals. d, e, f) Snapshots of reconstructed fish interactions (movie S7). The current fish position is marked by filled circles. Trailing dots indicate the positions over the preceding 5 s. Colors label individual fish throughout the manuscript. Large transparent circles denote occurrence of chirps. Gray dots indicate electrode positions, and light blue illustrates the water surface. d) Courting female (orange) and male (purple) are engaged in intense chirping activity. An intruder male (red) lingers at a distance of about one meter. e) The courting male attacks the intruder (purple arrow) who emits a series of chirps and, f) leaves the recording area (red arrow).

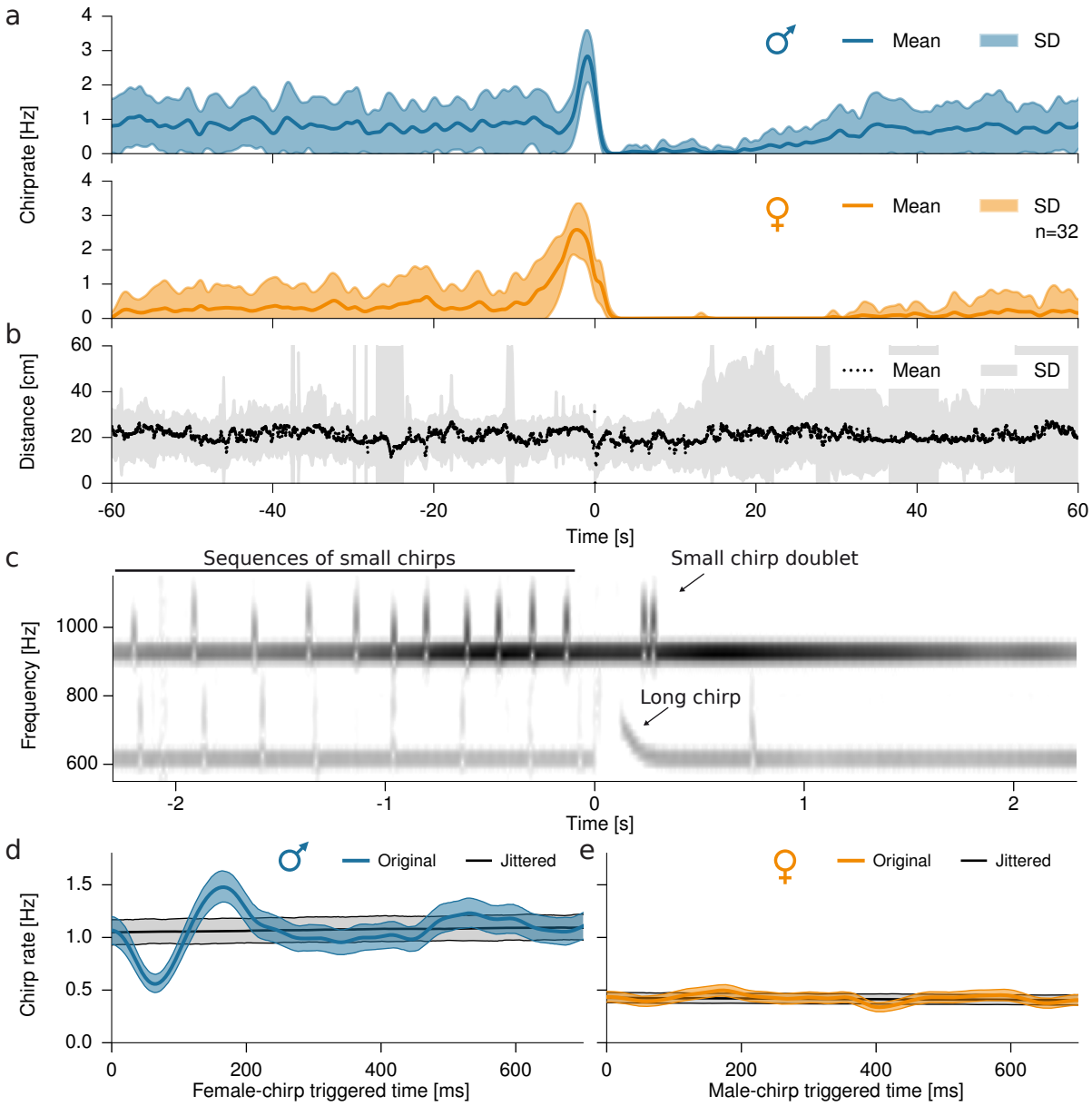

Figure 2: Temporal structure of courtship chirping of an example pair. a) Average rate of small chirps and b) distance between courting male and female fish before and after a female long chirp at time zero. Bands mark SD. c) Spectrogram (audio S5) shows EOD fs of a female (620 Hz) and male (930 Hz) during courtship and their stereotyped chirping pattern: the two fish concurrently produce series of small chirps before the female generates a long chirp and the male responds with a chirp-doublet. d, e) Chirp rate of one fish relative to each chirp of the other fish (cross-correlogram, median with 95 % inter-percentile range in color). Corresponding chirp rates from randomly jittered, independent chirp times in gray. d) Male chirping is first inhibited immediately after a female chirp (at 64 ms, Cohen's d = 9.3) and then transiently increased (at 166 ms after a chirp, d = 5.9). e) Female chirps are timed independently of male chirps (maximum d = 2.8).

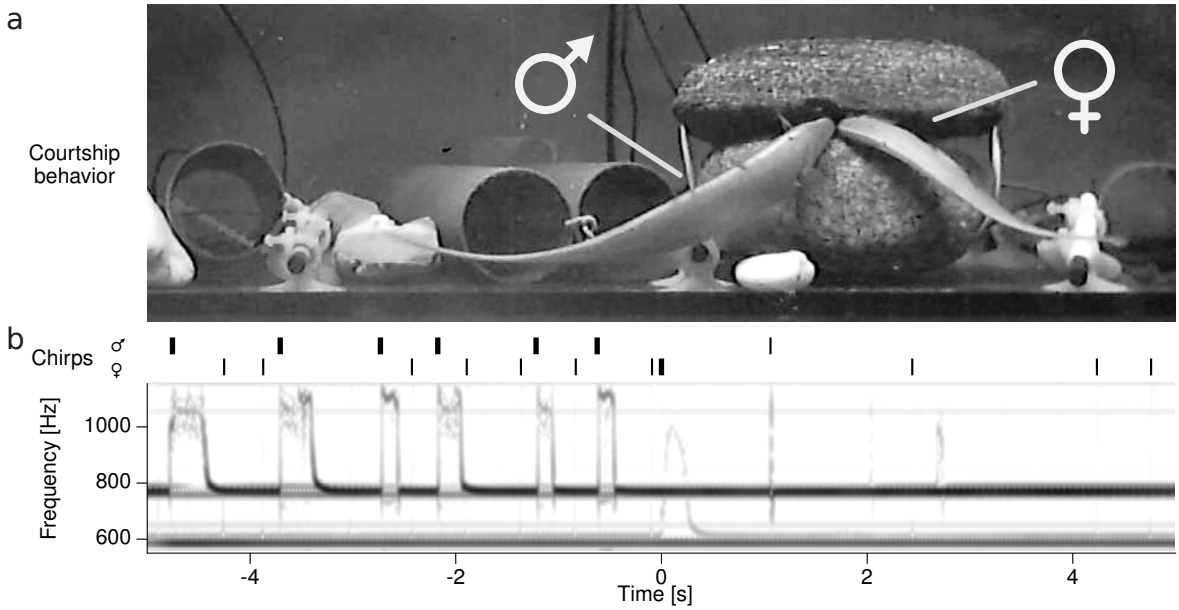

Figure 3: Synchronizing role of the female long chirp in spawning. a) Simultaneous video (snapshot of movie S9) and b) voltage recordings (spectrogram) of *A. leptorhynchus* in the lab demonstrate the synchronizing function of the female long chirp (at time zero; trace with 608 Hz baseline frequency) in spawning. In contrast to *A. rostratus,* male *A. leptorhynchus* generate an additional, long chirp type before spawning (top trace with 768 Hz baseline frequency). Chirp onset times of the male and the female are marked by vertical bars above the spectrogram. Thick and thin lines indicate long and short duration chirps, respectively.

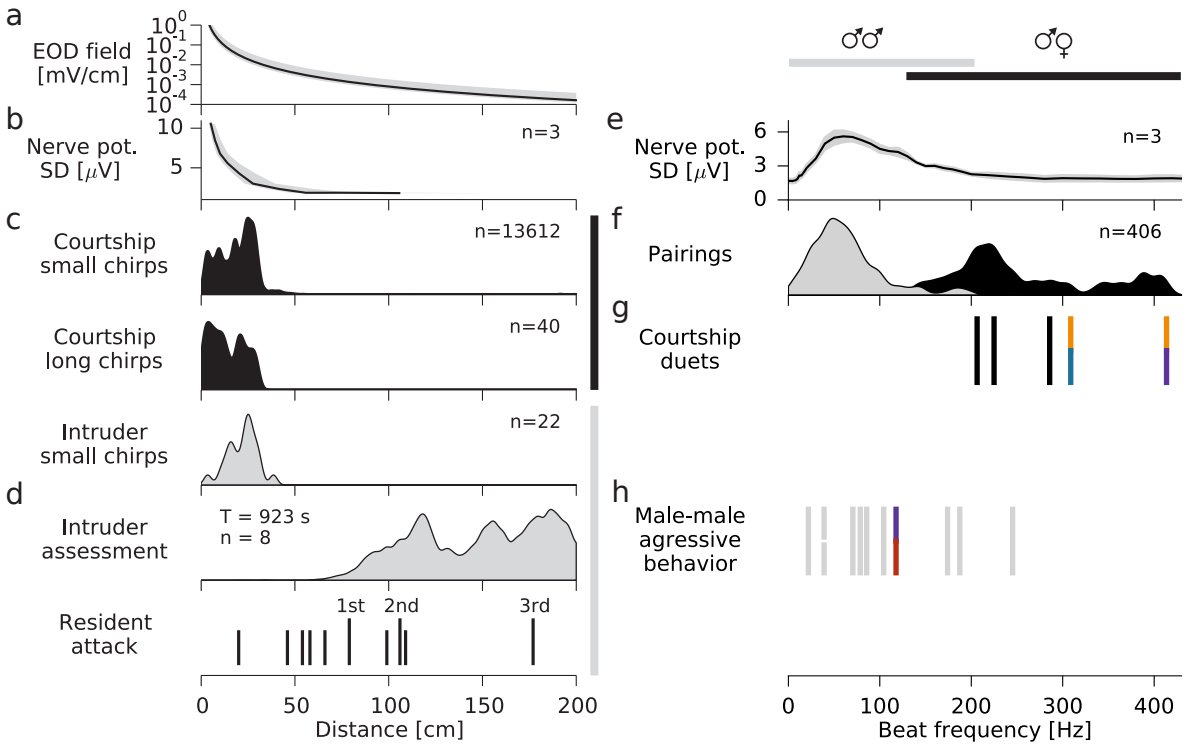

Figure 4: Non-optimal encoding. a) Maximum electric field strength as a function of distance from the emitting fish (median with total range). b) Activity of the electroreceptor population rapidly declines with distance between two fish (beat frequency 60 Hz). c) Small and long chirps in both courtship and aggression contexts are emitted consistently at distances below 32 cm. d) Intruder assessment and initiation of attacks by residents occur at much larger distances (movie S8). e) Tuning of electroreceptor activity to beat frequency. f) Distribution of beat frequencies of all *A. rostratus* appearing simultaneously in the electrode array. Gray: male-male, black: male-female (n = 439 pairings). g) Courtship behaviors occurred at beat frequencies in the range of 205–415 Hz, far from the receptors' best frequency. Colors indicate the scenes depicted above. h) Aggressive interactions occurred at beat frequencies below 245 Hz, better matching the tuning of the electroreceptors.

Supplemental information

Supplemental experimental procedures

Field site

The field site is located in the Tuira River basin, Province of Darién, Republic of Panamá (fig. S1 a), at Quebrada La Hoya, a narrow and slow-flowing creek supplying the Chucunaque River. Data were recorded about 2 km from the Emberá community of Peña Bijagual and about 5 km upstream of the stream's mouth (8°15'13.50"N, 77°42'49.40"W). The water of the creek is clear, but becomes turbid for several hours after heavy rainfall. The creek flows through a moist secondary tropical lowland forest, which, according to local residents, gets partially flooded on a regular basis during the wet season (May–November). The water levels of the creek typically range from 20–130 cm at different locations, but can rise temporarily to over 200 cm after heavy rainfall. At our recording site (fig. S1 b), the water level ranged from 20–70 cm. The banks of the creek are typically steep and excavated, consisting mostly of root masses of large trees. The water temperature varied between 25 and 27 °C on a daily basis and water conductivity was stable at 150–160 µS/cm. At this field site we recorded four species of weakly electric fish, the pulse-type fish *Brachyhypopomus occidentalis* (~ 30–100 Hz pulses per second), and the wave-type species *Sternopygus dariensis* (EOD*f* at ~ 40–220 Hz), *Eigenmannia humboldtii* (~ 200–600 Hz), and *Apteronotus rostratus* (~ 600–1100 Hz). We here focused exclusively on *A. rostratus*, a member of the *A. leptorhynchus* species group (brown ghost knifefish[1]) and its intraspecies interactions. Courtship interactions were observed after the onset of the rainy season in May and only in 2 out of 5 nights (Fig. S2).

Field monitoring system

Our recording system (Fig. 1 b, fig. S1 b) consisted of a custom-built 64-channel electrode and amplifier system (npi electronics GmbH, Tamm, Germany) running on 12 V car batteries. Electrodes were low-noise headstages encased in epoxy resin (1× gain, $10 \times 5 \times 5$ mm). Signals detected by the headstages were fed into the main amplifier (100× gain, 1st order high-pass filter 100 Hz, low-pass 10 kHz) and digitised with 20 kHz per channel with 16-bit amplitude resolution using a custom-built low-power-consumption computer with two digital-analog converter cards (PCI-6259, National Instruments, Austin, Texas, USA). Recordings were controlled with custom software written in C++ that also saved data to hard disk for offline analysis (exceeding 400 GB of uncompressed data per day). Raw signals and power spectra were monitored online

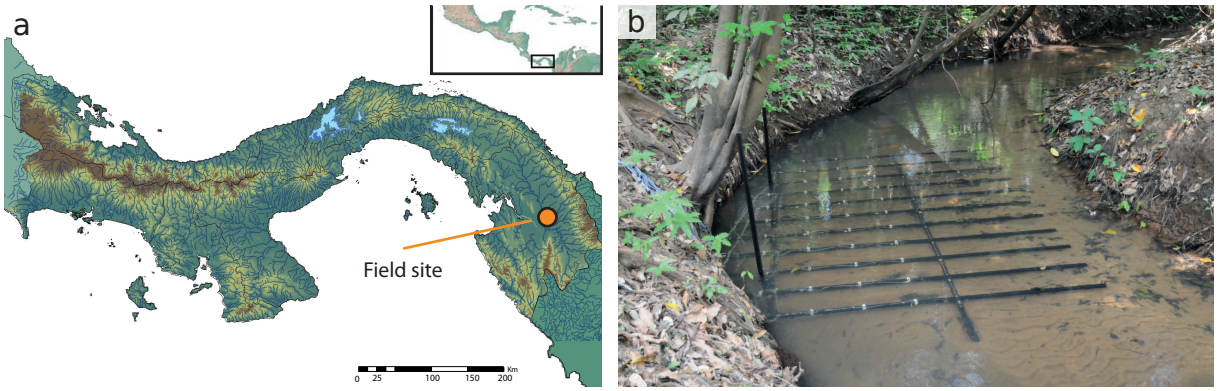

Figure S1: Field site and position of electrode array. A) The field data were recorded in the Darién province in Eastern Panamá. B) The electrode array covered $2.4 \times 1.5\,m^2$ of our recording site in a small quebrada of the Chucunaque River system. Electrodes (on white electrode holders) were positioned partly beneath the excavated banks, allowing to record electric fish hiding deep in the root masses.

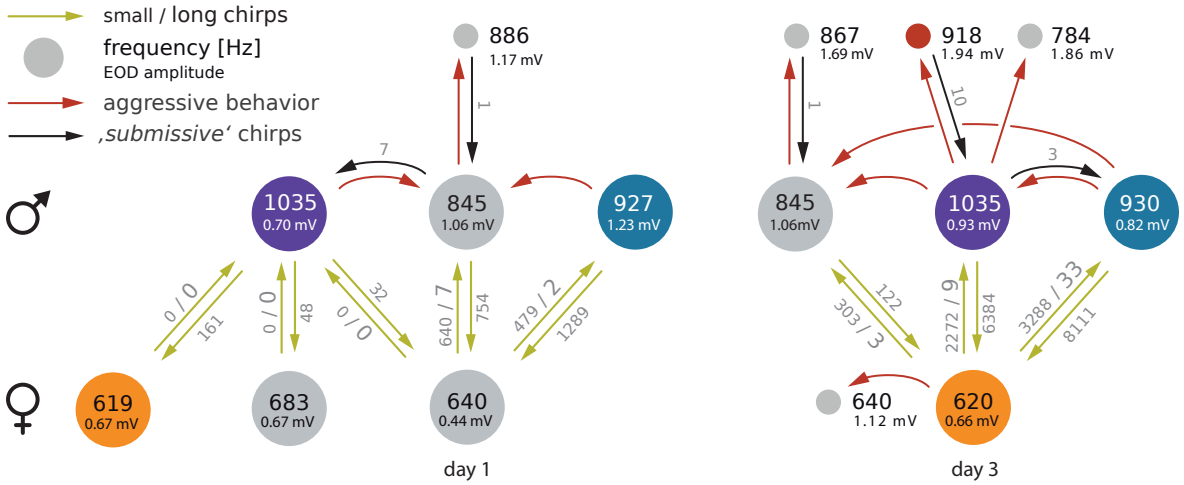

Figure S2: Ethogram of a selection of interacting *A. rostratus* individuals displaying their social relationships from two nights (2012-05-10 (day 1) and 2012-05-12 (day 3)). The numbers within shaded circles refer to the EODf (top, in Hz) and the EOD amplitude at 10 cm distance (bottom). Similar EODfs on day 1 and day 3 might indicate the same fish. Females were identified based on their low EOD frequency[2]. Green arrows and associated numbers indicate the numbers of small chirps and long chirps emitted in close proximity (< 50 cm). Red arrows indicate aggressive behaviors, and black arrows the number of small chirps emitted during aggressive interactions.

to ensure the quality of the recordings. We used a minimum of 54 electrodes, arranged in an 9×6 array covering an area of 240×150 cm (30 cm spacing). The electrodes were mounted on a rigid frame (thermoplast 4×4 cm profiles, 60 % polyamid, 40% fiberglass; Technoform Kunststoffprofile GmbH, Lohfelden, Germany), which was submerged into the stream and fixed in height 30 cm below the water level. Care was taken to position part of the electrode array below the undercut banks of the stream in order to capture the EODs of fish hiding in the root masses. The recording area covered about half of the width of the stream and the hiding places of several electric fish. The maximum uninterrupted recording time was limited to 14 hours, determined by the capacity of the car batteries (2×70 Ah) and the power consumption of the computer (22 W) and amplifier system (25 W). Facilities for charging the batteries were a bottleneck (solar power and gasoline-powered generators), therefore we focused on nighttime recordings. Gymnotiform species feature a cyclic reproduction controlled by environmental factors. In the tropics these factors are related to the transition from dry to wet season and include an increase in water level and a decrease in water conductivity [3]. We therefore recorded EODs during the transition from dry to wet season in February, March, and May 2012 and acquired a total of 162 hours of data.

Data analysis

All data analysis was performed in Python 2.7 (www.python.org). Summary data are expressed as means ± standard deviation, unless indicated otherwise.

Spectrograms Spectrograms in Fig. 2c and Fig. 3b were calculated from data sampled at 20 kHz in windows of 1024 and 2048 data points size, corresponding to 51.2 ms and 102.4 ms, respectively, applying a Blackman window function. Sequential windows were shifted by 50 data points (2.5 ms). The resulting spectrograms were interpolated in the frequency dimension for visual purposes using a resolution of 2 Hz and were then thresholded to remove low power background.

Fish identification and tracking Our EOD tracking system is optimized for identifying and tracking individual wave-type electric fish, to estimate the fish's positions, and to detect communication signals. The signals of pulse-type electric fish were detected, but remain unprocessed for now. First, information about electric fish presence, EOD frequency (EODf), and approximate position were extracted. Each electrode signal was analyzed separately in sequential overlapping windows (1.22 s width, 85 % overlap). For each window the power spectral density was calculated (8192 FFT data points, 5 sub-windows, 50% overlap) and spectral peaks above a given threshold were detected. Individual fish were extracted from the list of peak frequencies, based on the harmonic structure of wave-type EODs. For each analysis window, EOD detections from all electrodes were matched and consolidated. Finally, fish detections in successive time windows were matched, combined, and stored for further analysis. Slow EOD frequency modulations, so-called frequency rises [4], were already detected at this stage, but we observed only a single rise emitted by a retreating intruder fish.

Position estimation Once the presence of an electric fish was established, the fish's position was estimated and chirps were detected. For each fish, the signals of all electrodes were bandpass filtered (forward-backward butterworth filter, 3rd order, 5× multipass, ±7 Hz width) at the fish's EODf. Then the envelope was computed from the resulting filtered signal using a root-mean-square filter (10 EOD cycles width) and subsequent multiplication with $\sqrt{2}$. Each 40 ms the fish position $\vec{x}$ was estimated from the four electrodes i with the largest envelope amplitudes A_i at position $\vec{e_i}$ as a weighted spatial average

$$\vec{x} = \sum_{i=1}^{n=4} \sqrt{A_i} \cdot \vec{e_i} \tag{1}$$

(movie S6). If fewer than two electrodes with EOD amplitudes larger than 15 µV were available, the position estimate was omitted. Although this estimate does not relate to the underlying physics of the electric field, it proved to be the most robust against interference by electrical noise [5] and fish moving close to the edges of the electrode array, as verified with both experiments and simulations. For the electrode configuration used, the weighted spatial average yielded a precision of 4.2±2.6 cm on level with the electrode array and 6.2±3.8 cm at a vertical distance of 15 cm as computed by extensive simulations. Finally, the position estimates were filtered with a running average filter of 200 ms width to yield a smoother trace of movements. For pulse-type electric fish an EOD-based method for tracking electric fish position in shallow water in a laboratory setup has been published recently, yielding slightly better precision with a physically more realistic lookup-table-based approach [6].

Chirp detection and analysis For each fish the electrode voltage traces were bandpass-filtered (forward-backward butterworth filter, 3rd order, 5× multipass, ±7 Hz width) at the fish's EODf and at 10 Hz above the EODf. For each passband the signal envelope was estimated using a root-mean-square filter over 10 EOD cycles and subsequent multiplication with $\sqrt{2}$. Rapid positive EOD frequency excursions cause the signal envelope at the fish's baseline frequency to drop and in the passband above the fish's EODf to increase in synchrony with the frequency excursion. If events were detected synchronously in both passbands on more than two electrodes, and exceeded a preset amplitude threshold, they were accepted as communication signals.

Communication signals with a single peak in the upper passband were detected as small chirps. Signals of up to 600 ms duration and two peaks in the upper passband, marking the beginning and the end of the longer frequency modulation, were detected as long chirps. All chirps in this study were verified manually. However, it is likely that some chirps were missed, since detection thresholds were set such that the number of false positives was very low.

Interchirp-interval probability densities were generated for pairs of fish and only for the time period in which both fish were producing chirps. Kernel density histograms of interchirp intervals (fig. S3) were computed with a Gaussian kernel with a standard deviation of 20 ms.

Rates of small chirps before and after female long chirps (Fig. 2 a and fig. S4 a) were calculated by convolving the chirp times with a Gaussian kernel ($\sigma = 0.5$ s) separately for each episode and subsequently calculating the means and standard deviations.

For quantifying the echo response (Fig. 2 d, e and fig. S4 c, d) we computed the cross-correlogram

$$r(\tau) = \frac{1}{n_a} \sum_{j=1}^{n_a} \sum_{i=1}^{n_b} g(\tau - (t_{b,i} - t_{a,j})) \tag{2}$$

with the n_a chirp times $t_{a,j}$ of fish a and the n_b chirp times $t_{b,i}$ of fish b using a Gaussian kernel $g(t)$ with a standard deviation of 20 ms. To estimate its confidence intervals, we repeatedly resampled the original dataset (2000 times jackknife bootstrapping; random sampling with replacement), calculated the cross-correlogram as described above and determined the 2.5 and 97.5 % percentiles. To create the cross-correlograms of independent chirps, we repeatedly (2000 times) calculated the cross-correlograms on chirps jittered in time by adding a random number drawn from a Gaussian distribution with a standard deviation of 500 ms and determined the mean and the 2.5 and 97.5 % percentiles. We considered non-overlapping confidence intervalls, i.e., a separation by more than four standard deviations, as indicative of an echo response. Such large effects were observed for two pairs of fish in which many thousand chirps were generated. For three other pairs with with only a few hundred chirps, similar, but weaker effects were found.

Beat frequencies and spatial distances The distance between two fish at the time of each chirp (Fig. 4 c) was determined from the estimated fish positions. Because position estimates were not always available for each time point we allowed for a tolerance of maximally two seconds around the chirp for retrieving the position estimate. The positions were compiled into kernel density histograms that were normalized to their maximal value. The Gaussian kernel had a standard deviation of 1 cm for courtship small chirps, and 2 cm for courtship long chirps as well as intruder small chirps.

Males ($n = 8$) intruding on a courting dyad initially lingered at some distance from the dyad before either approaching the dyad further or being chased away by the courting resident male. Distances between the intruding male and the courting male during this assessment behavior (Fig. 4 d, top) were measured every 40 ms beginning with the appearance of the intruding fish until the eventual approach or attack. These distances, collected from a total assessment time of 923 s, were summarized in a kernel density histogram with Gaussian kernels with a standard deviation of 2 cm.

When a male intruded on a courting dyad it was directly attacked by the resident male. In that process courtship was always interrupted and eventually one of the males withdrew. In some cases a few chirps were emitted by the retreating male. The winning male always approached and courted the female. The attack distances between two males (Fig. 4 d, bottom) were determined at the moment a resident male initiated its movement toward an intruding male. This moment was clearly identifiable as the onset of a linear movement of the resident male towards the intruder from plots showing the position of the fish as a function of time.

The distribution of beat frequencies generated by fish present in the electrode array at the same time (Fig. 4 f) was calculated from all available recordings during the breeding season. The average frequency difference of each pair of fish simultaneously detected in the recordings was compiled into a kernel density histogram with a Gaussian kernel with a standard deviation of 10 Hz. Similarly, for courtship and aggressive behavior (Fig. 4 g, h) the mean frequency differences were extracted for the duration of these interactions.

Electric fields For an estimation of EOD amplitude as a function of distance, histograms of envelope amplitudes from all electrodes of the array were computed as a function of distance between the electrodes and the estimated fish position. For each distance bin in the range of 20–100 cm the upper 95 % percentile of the histogram was determined and a power law was fitted to these data points. Gymnotiform electroreceptors measure the electric field, i.e. the first spatial derivative of the EOD amplitudes as shown in Fig. 4 a.

Breeding monitoring setup

In the laboratory breeding study, we used the brown ghost knifefish *Apteronotus leptorhynchus*, a close relative of *A. rostratus* [1]. *Apteronotus leptorhynchus* is an established model organism in neuroscience and readily available from aquarium suppliers. The two species share many similarities. (i) Most chirps produced by both species are "small chirps" that in *A. leptorhynchus* have been classified as type-2 chirps [7]. (ii) Females of both species additionally generate small proportions of "long chirps", similar to the type-4 chirps classified for *A. leptorhynchus* males. (iii) Both species show the same sexual dimorphism in EODf.

The laboratory setup for breeding *A. leptorhynchus* consisted of a holding tank ($100 \times 45 \times 60$ cm) placed in a darkened room and equipped with bubble filters and PVC tubes provided for shelter. Heating was supplied via room temperature, which kept water temperature between 21 and 30 °C. The light/dark cycle was set to 12/12 hours. Several pieces of rock were placed in the center of the tank as spawning substrate. EOD signals were recorded differentially using four pairs of graphite electrodes. Two electrode pairs were placed on each side of the spawning substrate. The signals were amplified and analog filtered using a custom-built amplifier (100× gain, 100 Hz high-pass, 10 kHz low-pass; npi electronics GmbH, Tamm, Germany), digitized at 20 kHz with 16 bit (PCI-6229, National Instruments, Austin, Texas, USA), and saved to hard disk for offline analysis. The electrode pairs were positioned orthogonally to each other, thereby allowing for robust recordings of EODs independent of fish orientation. The tank was illuminated at night with a dozen infrared LED spotlights (850 nm, 6W, ABUS TV6700) and monitored continuously (movie S9) with two infrared-sensitive high-resolution video cameras (Logitech HD webcam C310, IR filter removed manually). The cameras were controlled with custom written software (https://github.com/bendalab/videoRecorder) and a timestamp for each frame was saved for later synchronisation of the cameras and EOD recordings. Six fish of *A. leptorhynchus* (three male, three female; imported from the Río Meta region, Columbia) were kept in a tank for over a year before being transferred to the recording tank. First, fish were monitored for about a month without external interference. We then induced breeding conditions [3] by slowly lowering water conductivity from 830 µS/cm to about 100 µS/cm over the course of three months by diluting continuously the tank water with deionized water. The tank was monitored regularly for the occurrence of spawned eggs.

Electrophysiology

For *in vivo* recordings fish were anesthetized with MS-222 (120 mg/l; PharmaQ, Fordingbridge, UK; buffered to pH 7 with sodium bicarbonate) and a small part of the skin was removed to expose the anterior part of the lateral line nerve that contains only electroreceptor afferent fibers innervating electroreceptors on the fish's trunk [8]. The margin of the wound was treated with the local anesthetic Lidocaine (2%; bela-pharm, Vechta, Germany). Then the fish was immobilized by intramuscular injection of Tubocurarine (Sigma-Aldrich, Steinheim, Germany; 25–50 µl of 5 mg/ml solution), placed in a tank, and respired by a constant flow of water through its mouth. The water in the experimental tank ($47 \times 42 \times 12$ cm) was from the fish's home tank with a conductivity of about 300 µS/cm and kept at 28 °C. All experimental protocols were approved by the local district animal care committee and complied with federal and state laws of Germany (file no. ZP 1/13) and Canada.

Population activity in whole-nerve recordings was measured using a pair of hook electrodes of chlorided silver wire. Signals were differentially amplified (gain 10 000) and band-pass filtered (3 to 3 000 Hz passband, DPA2-FX; npi electronics), digitized (20 kHz sampling rate, 16-bit, NI PCI-6229; National Instruments), and recorded with RELACS (www.relacs.net) using efield and efish plugins. The strong EOD artifact in this kind of recording was eliminated before further analysis by applying a running average of the size of one EOD period [9]. The resulting signal roughly followed the amplitude modulation of the EOD and we quantified its amplitude by taking its standard deviation. The nerve recordings closely resemble the properties of P-unit responses obtained from single and dual-unit recordings [9, 10]. Note, however, that P-units might still respond in subtle ways to a stimulus even though the nerve recording is already down at baseline level, because of additional noise sources in this kind of recording. Signal-to-noise ratios were simply computed as Cohen's d between the responses and baseline activity.

Electric sine-wave stimuli with frequencies ranging from $\Delta f = -460$ to $+460$ Hz in steps of 2 Hz ($|\Delta f| \leq 20$ Hz), 10 Hz ($|\Delta f| \leq 200$ Hz), and 20 Hz ($|\Delta f| > 200$ Hz) relative to the fish's EODf were applied through a pair of stimulation electrodes (carbon rods, 30 cm long, 8 mm diameter) placed on either side of the fish. Stimuli were computer-generated and passed to the stimulation electrodes after being attenuated to the right amplitude (0.05, 0.1, 0.2, 0.5, 1.0, 2.5, 5.0, 10.0, 20.0, 40.0 % of the fish's EOD amplitude estimated with a pair of electrodes separated by 1 cm perpendicular to the side of the fish) and isolated from ground (Attenuator: ATN-01M; Isolator: ISO-02V; npi electronics). For more details see [9, 10].

Tuning mismatch

The frequency mismatch between the tuning of the electroreceptor population and the high beat frequencies occurring during courtship is unexpected and immediately raises fundamental questions about the encoding of electrosensory signals. Are there additional sensory pathways that could convey these signals? Could subpopulations of receptor units be better matched to the high beat frequencies? How are these signals decoded by downstream neurons? Might the frequency tuning of the receptor neurons be regulated by sexual hormones? Before addressing these issues, let us clarify that the observed mismatch does not imply that no information is transmitted about high beat frequencies. The receptor population is activated, but at a weak activity level at the tail of its tuning curve.

Potentially relevant types of receptor neurons: Gymnotiform weakly electric fish have three types of electroreceptor cells: (i) Ampullary receptors that are tuned to low-frequency (< 50 Hz) external electric fields emitted by, for example, muscle activity of potential prey objects[11]. The EOD with its EODf of more than about 600 Hz does not stimulate ampullary neurons. In addition, chirps in *Apteronotus* have no low-frequency component and thus do not stimulate ampullary receptors in contrast to different types of chirps in *Eigenmannia* [12, 13]. (ii) T-units are tuberous receptors that fire one action potential on every EOD cycle[14]. The T-unit population encodes sub-microsecond phase shifts induced by beats and are used by *Eigenmannia* to disambiguate the sign of the beat in the context of the jamming avoidance response (JAR) occurring at beat frequencies below about 15 Hz[15, 16]. However, the JAR of *Apteronotus* is independent of the sign of the beat[17] and T-units are much rarer in *Apteronotus* than in *Eigenmannia* [18, 19]. Also, in Eigenmannia T-units are more narrowly tuned to the fish's EODf making them less sensitive to EODfs of other fish than P-units[20]. In summary, T-units appear to play a minor role in *Apteronotus* and it is unlikely that they are able to encode high frequency beats. (iii) P-units, the second and dominant type of tuberous receptors, encode amplitude modulations of the fish's EOD in their firing rate[14, 21, 22].

P-unit tuning and sensitivity: The tuning of P-units to beat frequencies has been characterized up to 300 Hz by single unit recordings in both *A. albifrons* and *A. leptorhynchus[9, 10, 21].* All studies agree that the average P-unit response is strongest at beat frequencies of about 50 to 100 Hz and declines almost back to baseline levels at 300 Hz in accordance with the measurement we show in Fig. 4 e.

P-units are heterogeneous in their baseline activity[23, 24]. Basic properties of spiking neurons suggest that frequency tuning mainly depends on baseline firing rate[25]. Therefore P-units with high baseline rates might have a frequency tuning that extends to higher frequencies than the average tuning of the population. This is supported by noticeable stimulus-response coherences that have been measured with narrowband noise stimuli up to 400 Hz[24].

Most of these studies used rather strong beat amplitudes of more than 10 % of the EOD amplitude. We observed chirp interactions at distances up to 32 cm, corresponding to beat amplitudes from 100 % down to about 1 % of the EOD amplitude. Smaller beat amplitudes result in down-scaled frequency tuning curves[9, 21]. In particular for amplitudes below 10 % responses to beat frequencies larger than 200 Hz are getting close to baseline activity.

Chirp encoding can be understood based on the frequency tuning of P-units[10]. A chirp transiently changes the beat frequency. The response to the chirp differs only as much from the response to the background beat as the frequency response to the chirp differs from the one to the beat. Therefore we expect chirp coding to be impaired by the low slope of the P-unit's frequency tuning curve at high beat frequencies.

Decoding: P-units converge onto pyramidal cells in the electrosensory lateral line lobe (ELL)[19, 26, 27]. The pyramidal cells processing communication signals[28, 29, 30] integrate over about 1000 P-units[27]. To our knowledge convergence onto pyramidal cells is not selective; pyramidal cells average over the P-unit population irrespective of their baseline firing rate and tuning range. This is supported by the tuning curves measured in pyramidal cells that peak at frequencies similar or lower than the P-units[26]. Stimulus-response coherences of pyramidal cells peak well below 100 Hz, but have only been measured up to 120 Hz[29, 30, 31]. Coding of small chirps by pyramidal cells in the ELL has so far only been studied at beat frequencies below 60 Hz[32, 33].

Hormonal state: Depending on the state of the animal the P-unit tuning may be modified, e.g., by hormones and/or neuromodulators[34]. Steroids are known to modulate EODf and tuning of P-units to EODf [2, 35, 36]. Serotonin enhances activity levels in ELL[37] and cholinergic activation of muscarinic receptors improve low frequency coding of pyramidal cells[38]. Whether and how hormones or neuromodulators influence coding of high-frequency beats is not known yet.

Conclusion: P-units are the only relevant receptor type involved in encoding high beat frequencies. Average P-unit tuning is similar in different species. Frequency tuning in P-units declines beyond about 100 Hz, but some P-units do encode beat frequencies higher than 300 Hz, in particular at high beat amplitudes occurring below about 10 cm distance between the two interacting fish. The strong frequency mismatch we observe in our data (Fig. 4) is therefore not completely enigmatic: courtship signals could potentially be encoded by at least a subpopulation of P-unit electroreceptors. However, an unknown selection pressure generated a strong EODf dimorphism that pushes the courtship signals towards the tail of the receptor tuning curve, such that the resulting stimulus distribution (Fig. 4f) is not matched by the receptor tuning (Fig. 4e) to maximize information transmission.

References

[1] de Santana, C. D. and Vari, R. P. (2013). Brown ghost electric fishes of the *Apteronotus leptorhynchus* species-group (Ostariophysi, Gymnotiformes); monophyly, major clades, and revision. *Zool J Linnean Soc* 168, pp. 564–596.

[2] Meyer, J., Leong, M., and Keller, C. (1987). Hormone-induced and maturational changes in electric organ discharges and electroreceptor tuning in the weakly electric fish *Apteronotus*. *J Comp Physiol A* 160, pp. 385–394.

[3] Kirschbaum, F. and Schugardt, C. (2002). Reproductive strategies and developmental aspects in mormyrid and gymnotiform fishes. *J Physiol Paris* 96, pp. 557–566.

[4] Zakon, H., Oestreich, J., Tallarovic, S., and Triefenbach, F. (2002). EOD modulations of brown ghost electric fish: JARs, chirps, rises, and dips. *J Physiol Paris* 96.5–6, pp. 451–458.

[5] Hopkins, C. (1973). Lightning as background noise for communication among electric fish. *Nature* 242.5395, pp. 268–270.

[6] Jun, J., Longtin, A., and Maler, L. (2013). Real-Time Localization of Moving Dipole Sources for Tracking Multiple Free-Swimming Weakly Electric Fish. *PLoS ONE* 8.6.

[7] Engler, G. and Zupanc, G. (2001). Differential production of chirping behavior evoked by electrical stimulation of the weakly electric fish, *Apteronotus leptorhynchus*. *J Comp Physiol A* 187.9, pp. 747–756.

[8] Maler, L., Finger, T., and Karten, H. (1974). Differential projections of ordinary lateral line receptors and electroreceptors in the gymnotid fish, *Apteronotus (Sternarchus) albifrons*. *J Comp Neurol* 158, pp. 363–382.

[9] Benda, J., Longtin, A., and Maler, L. (2006). A Synchronization-Desynchronization Code for Natural Communication Signals. *Neuron* 52, pp. 347–358.

[10] Walz, H., Grewe, J., and Benda, J. (2014). Static frequency tuning properties account for changes in neural synchrony evoked by transient communication signals. *J Neurophysiol* 112, pp. 752–765.

[11] Kalminj, A. (1974). The detection of electric fields from inanimate and animate sources other than electric organs. *Electroreceptors and Other Specialized Receptors in Lower Vertrebrates.* Ed. by A. Fessard. Vol. 3. Handbook of Sensory Physiology. Springer, pp. 148–200.

[12] Metzner, W. and Heiligenberg, W. (1991). The coding of signals in the electric communication of the gymnotiform fish *Eigenmannia*: From electroreceptors to neurons in the torus semicircularis of the midbrain. *J Comp Physiol A* 169, pp. 135–150.

[13] Stöckl, A., Sinz, F., Benda, J., and Grewe, J. (2014). Encoding of social signals in all three electrosensory pathways of *Eigenmannia virescens*. *J Neurophysiol* 112, pp. 2076–2091.

[14] Scheich, H., Bullock, T. H., and Robert H. Hamstra, J. (1973). Coding properties of two classes of afferent nerve fibers: high frequency electroreceptors in the electric fish, *Eigenmannia*. *J Neurophysiol* 36, pp. 39–60.

[15] Bullock, T., H, R., and Scheich, H. (1972). The jamming avoidance response of high frequency electric fish. II. Quantitative aspects. *J Comp Physiol* 77.1, pp. 23–48.

[16] Rose, G. and Heiligenberg, W. (1985). Temporal hyperacuity in the electric sense of fish. *Nature* 318, pp. 178–180.

[17] Heiligenberg, W., Wong, C. J. H., Metzner, W., and Keller, C. H. (1996). Motor control of the jamming avoidance response of *Apteronotus leptorhynchus*: evolutionary changes of a behavior and its neuronal substrates. *J Comp Physiol A* 179, pp. 653–674.

[18] Maler, L., Sas, E. K. B., and Rogers, J. (1981). The cytology of the posterior lateral line lobe of high-frequency weakly electric fish (Gymnotidae): Dendritic differentiation and synaptic specificity in a simple cortex. *J Comp Neurol* 195, pp. 87–139.

[19] Heiligenberg, W. and Dye, J. (1982). Labelling of Eleetroreeeptive Afferents in a Gymnotoid Fish by Intraeellular Injection of HRP: The Mystery of Multiple Maps. *J Comp Physiol* 148, pp. 287–296.

[20] Hopkins, C. D. (1976). Stimulus filtering and electroreception: Tuberous electroreceptors in three species of gymnotoid fish. *J Comp Physiol A* 111, pp. 171–207.

[21] Bastian, J. (1981a). Electrolocation I. How Electroreceptors of *Apteronotus albifrons* Code for Moving Objects and Other Electrical Stimuli. *J Comp Physiol* 144, pp. 465–479.

[22] Nelson, M., Xu, Z., and Payne, J. (1997). Characterization and modeling of P-type electrosensory afferent responses to amplitude modulations in a wave-type electric fish. *J Comp Physiol A* 181, pp. 532–544.

[23] Gussin, D., Benda, J., and Maler, L. (2007). Limits of linear rate coding of dynamic stimuli by electroreceptor afferents. *J Neurophysiol* 97, pp. 2917–2929.

[24] Savard, M., Krahe, R., and Chacron, M. J. (2011). Neural heterogeneities influence envelope and temporal coding at the sensory periphery. *Neurosci* 172, pp. 270–284.

[25] Knight, B. W. (1972). Dynamics of Encoding in a Population of Neurons. *J Gen Physiol* 59, pp. 734–766.

[26] Bastian, J. (1981b). Electrolocation II. The Effects of Moving Objects and Other Electrical Stimuli on the Activities of Two Categories of Posterior Lateral Line Lobe Cells in *Apteronotus albifrons*. *J Comp Physiol* 144, pp. 481–494.

[27] Maler, L. (2009). Receptive field organization across multiple electrosensory maps. I. Columnar organization and estimation of receptive field size. *J Comp Neurol* 516, pp. 376–393.

[28] Metzner, W. and Juranek, J. (1997). A sensory brain map for each behavior? *PNAS* 94, pp. 14798–14803.

[29] Chacron, M. J., Doiron, B., Maler, L., Longtin, A., and Bastian, J. (2003). Non-classical receptive field mediates switch in a sensory neuron's frequency tuning. *Nature* 423, pp. 77–81.

[30] Krahe, R., Bastian, J., and Chacron, M. (2008). Temporal processing across multiple topographic maps in the electrosensory system. *J Neurophysiol* 100.2, pp. 852–867.

[31] Chacron, M. J. (2006). Nonlinear information processing in a model sensory system. *J Neurophysiol* 95, pp. 2933–2946.

[32] Vonderschen, K. and Chacron, M. J. (2011). Sparse and dense coding of natural stimuli by distinct midbrain neuron subpopulations in weakly electric fish. *J Neurophysiol* 106, pp. 3102–3118.

[33] Marsat, G., Longtin, A., and Maler, L. (2012). Cellular and circuit properties supporting different sensory coding strategies in electric fish and other systems. *Curr Opin Neurobiol* 22, pp. 1–7.

[34] Márquez, B. T., Krahe, R., and Chacron, M. J. (2013). Neuromodulation of early electrosensory processing in gymnotiform weakly electric fish . *J Exp Biol* 216, pp. 2442–2450.

[35] Meyer, J. and Zakon, H. (1982). Androgens alter the tuning of electroreceptors. *Science* 217, pp. 635–637.

[36] Dunlap, K., Thomas, P., and Zakon, H. (1998). Diversity of sexual dimorphism in electrocommunication signals and its androgen regulation in a genus of electric fish, *Apteronotus*. *J Comp Physiol A* 183.1, pp. 77–86.

[37] Deemyad, T., Metzen, M. G., Pan, Y., and Chacron, M. J. (2013). Serotonin selectively enhances perception and sensory neural response to stimuli generated by same sex conspecifics. *PNAS* 110.48, pp. 19609–19614.

[38] Ellis, L. D., Krahe, R., Bourque, C. W., Dunn, R. J., and Chacron, M. J. (2007). Muscarinic Receptors Control Frequency Tuning Through the Downregulation of an A-Type Potassium Current. *J Neurophysiol* 98, pp. 1526–1537.

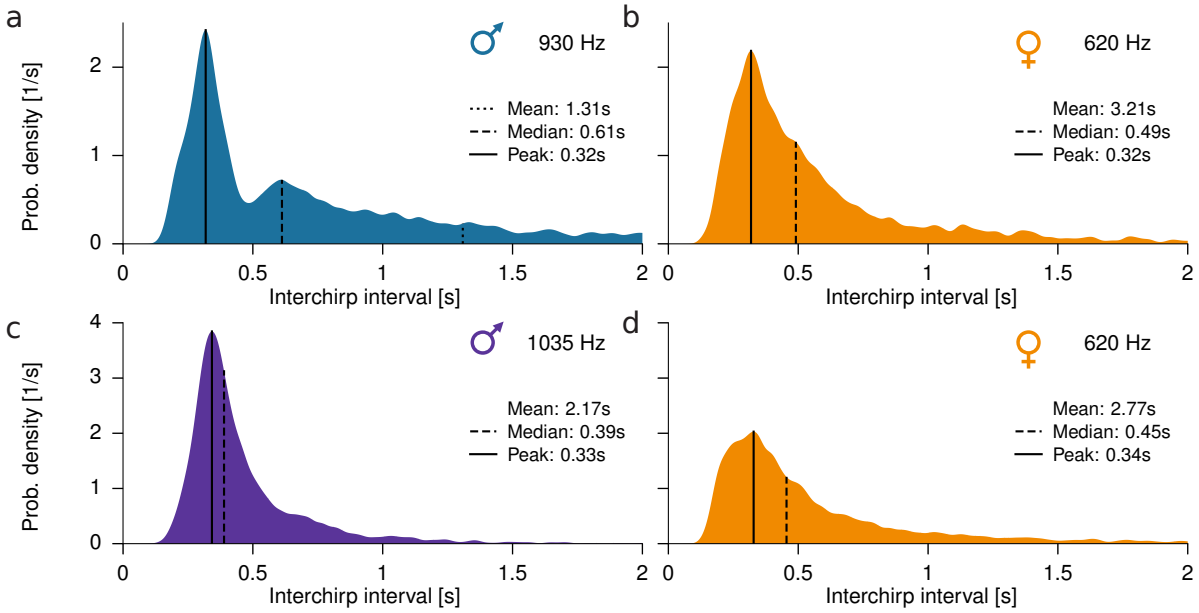

Figure S3: Interchirp-interval distributions of small chirps of an example female (right column, EODf = 620 Hz; B: n = 3431, D: n = 5336 chirps) interacting with two males (left column; A: EODf = 930 Hz, n = 8439; C: EODf = 1035 Hz, n = 6857 chirps).

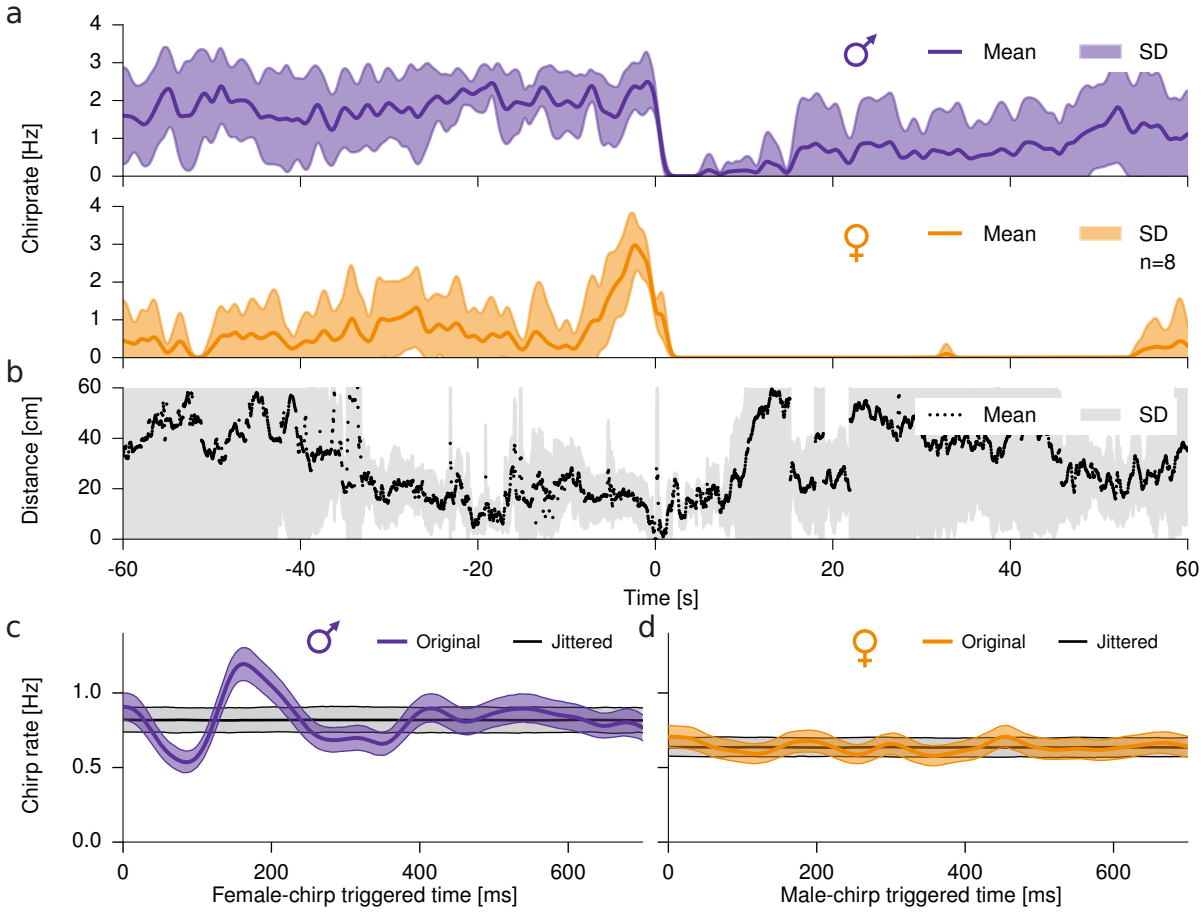

Figure S4: Temporal structure of courtship chirping for a second pair of fish. A) The average rate of small chirps and B) the distance between a courting male and female fish before and after a female long chirp at time zero. Gray bands mark standard deviation. Here the male (purple) is chirping continuously with an elevated rate before the long chirp is emitted by the female (orange). Note the reduction in distance and the reduced standard deviation of distance around time zero, the presumed time of spawning. C, D) Chirp rate of one fish relative to each chirp of the other fish (cross-correlogram, median with 95 % inter-percentile range in color). Corresponding chirp rates from randomly jittered, independent chirp times are displayed in gray. C) Male chirping is first inhibited immediately after a female chirp (at 85 ms, Cohen's $d = 7.1$) and then transiently increased (at 162 ms after a chirp, $d = 7.5$). D) Female chirps are timed independently of the male chirps ($d < 2.0$).

Audio, Animations, and Video

Audio S5: Audio trace of the courtship sequence shown in Fig. 2 c. A male (930 Hz) generated a series of small chirps. Eventually, the female (620 Hz) fish joins in, increases chirp rate and finishes with a long chirp, which is acknowledged by the male with a small chirp doublet.

File: audio_courtship.wav

Movie S6: Example of raw voltage recordings and corresponding position estimates of a single fish, *Eigenmannia humboldtii*, passing through the array of electrodes. The head and tail area of its electric field are of opposite polarity, which is why the polarity of the recorded EOD switches as the fish passes an electrode. Note the large electric spikes occurring irregularly on all electrodes. Previous studies [5] attributed similar patterns to propagating distant lightning. The animation is played back at real-time.

File: movie_raw_and_position.mp4

Movie S7: Animation of the courtship and aggression behavior shown in Fig. 1 d – f. A courting dyad is engaged in intense chirp activity (transparent circles and 50 ms beeps at the fish's baseline EODf). An intruder male (red circles indicate positions of the last 5 seconds, black circles mark current positions) first lingers at a distance of one meter. When it approaches further, courting is interrupted and the resident male engages the intruder. Just before the male intruder retreats, it emits a series of small chirps, and subsequently leaves the recording area. The resident male returns to the female and resumes chirping. Eventually, the female responds with small chirps followed by a single long chirp (large open circle and a 500 ms beep at the female's baseline EODf). Then both fish cease chirp activity and the male resumes to emit chirps after a few seconds. The animation is played back at 2× real-time.

File: movie_intruder.mp4

Movie S8: Animation of a courtship sequence with multiple attempts of an intruding male to approach the courting dyad. The resident male drives the intruder away three times , starting the approach at increasingly greater distances (marked in Fig. 4 d, bottom, no. 1–3). *Apteronotus rostratus* are marked by circles, *Eigenmannia humboldtii* by squares. The animation is played back at 2× real-time.

File: movie_repetitive_intruder.mp4

Movie S9: Spawning of the closely related species *Apteronotus lepthorhynchus* during a breeding experiment. The overall sequence of chirp production is very similar to the courtship motif observed in *A. rostratus*. However, male *A. lepthorhynchus* increasingly generate a second type of chirp, a variety of a long chirp, as spawning approaches. The video shows a big male (EODf = 770 Hz) courting a smaller female (590 Hz). The audio signal was created from concurrent EOD recordings. Both fish generate chirps at an increased rate (about 1.5 Hz), just before the male thrusts its snout against the female, which responds with a long chirp, clearly noticeable from the audio trace. Subsequently, the male retreats to a tube and the female hovers around the substrate, where the spawned egg was found.

File: movie_spawning.mp4